ELSEVIER

Journal of Contaminant Hydrology 31 (1998) 337–348

JOURNAL OF
Contaminant
Hydrology

Visualization by light transmission of oil and water contents in transient two-phase flow fields

Christophe J.G. Darnault, James A. Throop, David A. DiCarlo, Alon Rimmer, Tammo S. Steenhuis *, J.-Yves Parlange

Department of Agricultural and Biological Engineering, Cornell University, Ithaca, NY 14853, USA

Received 26 November 1996; revised 29 August 1997; accepted 29 August 1997

Abstract

The difficulty of determining transient fluid contents in a soil–oil–water system is hampering an understanding of the system's flow characteristics. In this paper, we describe a light transmission method (LTM) which can rapidly obtain oil and water contents throughout a large two-dimensional flow field of silica sand. By appropriately coloring the water with 0.005% FD&C blue #1, the hue of the transmitted light is found to be directly related to the water content within the porous media. The hue provides a high resolution measurement of the water and oil contents in transient flow fields (such as unstable flow). Evaluation of the reliability of LTM was assessed by checking the mass balance for a known water injection and its utility in visualizing a whole flow field was exemplified for unstable fingered flow by comparing fluid contents to those obtained with synchrotron X-ray radiation. © 1998 Elsevier Science B.V.

Keywords: Light Transmission Method (LTM); Silica sand; Transient flow

1. Introduction

The complexity of simultaneous flow of water and non-aqueous phase liquids (NAPLs) is little understood because few techniques permit accurate measurement of water and oil contents in transient flow fields. Mercer and Cohen (1990) noted that in situ fluid content measurements are needed to understand immiscible fluid flows in porous media and to perform effective subsurface remediation.

* Corresponding author. Department of Agricultural and Biological Engineering, Riley–Robb Hall, Cornell University, Ithaca, NY, USA 14853. Tel.: +1-607-255-2489; fax: +1-607-255-4080; e-mail: tss1@cornell.edu

PII S0169-7722(97)00068-5

Most techniques available for measuring oil and water fluid contents can be used only near steady state flow conditions. They include conventional X-ray and gamma ray radiation techniques used by Hopmans and Dane (1986), Lenhard et al. (1988), Dane et al. (1992), and Illangasekare et al. (1995), among others. These measurements are slow because of the relatively long counting times and only one point can be measured at one time. Synchrotron X-rays (Liu et al., 1993; Rimmer et al., 1998) allow shorter counting times (in the order of seconds) but only regions of less than 0.5 cm^2 can be measured at one time. Tidwell and Glass (1994) have performed full field measurements using X-ray film, but recording times are too long for measuring transient flow phenomena.

Transient visualizations (but not a direct measurement of fluid contents) have been made in Hele–Shaw cells with smooth walls (Saffman and Taylor, 1958; Chuoke et al., 1959) or with imprints of porous media on glass (Schwille, 1988). The visualization method of Van Geel and Sykes (1994) allows the measurement of liquid content near the wall of the slab chambers by relating the gray level of the reflected light to water content. However, as they noted, the fluid content near the wall might not necessarily be the same as within the porous media.

Thus, there is a need for a method that allows full field moisture content visualization in two-phase liquid systems. This paper describes the development of such a technique by using light transmission through a two-dimensional slab chamber. By coloring the water phase with 0.005% FD&C blue #1 the hue value of the transmitted light is directly related to the water content. The technique is a new application of the method of Glass et al. (1989) for air–water systems in which the light intensity was directly related to water content. Unlike air and water, in the case of oil–water systems the refractive index of the two fluids is almost identical, making it impossible to measure liquid contents of each of the fluids from the light intensity measurements. A blue dye was chosen because it produced a wide color spectrum going from yellow for the oil-saturated sand via green to blue for water-saturated soil.

2. Visualization

Quantification of color differences can be complicated, because there are various ways to specify color. The color for video cameras, color monitors and computer graphics is defined in terms of a vector with the three components of red, green and blue intensities (RGB). Another system to specify the color vector involves hue, saturation and intensity (HSI), which is used, for instance, by the Munsell color chart for soil classification. Hue is the attribute that describes the pure color and is what we are typically referring to when we use the term color. Saturation is the attribute that describes the degree to which the color is diluted with white. Intensity is the attribute which corresponds to the gray level (black and white) of the color image. The advantages of the HSI format are that it treats color roughly the same way that humans perceive and interpret color. Therefore, because color differences are apparent to the human eye for different water and oil contents, we expect that water content is directly related with hue rather than intensity or saturation.

Hue, H, in HSI format can be obtained from the RGB vector (R = red, G = green and B = blue intensity, respectively, with values for each vector component ranging from 0 to 255) following (Wilson, 1988):

$$H = 255\left[\frac{1}{360}\left[\Upsilon - \mathrm{ARCTAN}\frac{2\mathrm{R}-\mathrm{G}-\mathrm{B}}{\sqrt{3}\,(\mathrm{G}-\mathrm{B})}\right]\right], \quad (1)$$

where $\Upsilon = 90$ for $\mathrm{G} \geq \mathrm{B}$, $\Upsilon = 270$ for $\mathrm{G} < \mathrm{B}$,

where Υ is a constant depending on the green and blue intensity. This equation shows that if, as we expect, H is the best variable to measure water content, each of the components of the RGB vector is affected by the water content and the combination $(2\mathrm{R}-\mathrm{G}-\mathrm{B})/(\mathrm{G}-\mathrm{B})$ would be the relevant parameter in the RGB system to relate to water content.

3. Materials and methods

For fluid content measurements in porous media, light transmission techniques involve placing a two-dimensional experimental chamber in front of a uniform light source and recording the transmitted light (Glass and Nicholl, 1995). We used a light source composed of a bank of 24 high frequency fluorescent light bulbs in front of a white background. Experimental chambers had 1 cm thick polycarbonate walls with a 1 cm thick interior. The transmitted light was recorded with a Cohu Solid State Color Camera located 1 m in front of the chamber, with constant settings (zoom = 3–5 m and aperture = f 1.8) and stored on standard VHS tape in RGB format. Recorded images were converted from RGB to HSI format with an IBM compatible computer equipped with a DT2871 Color Frame Grabber and analyzed with a SP0228 V1.00 Color Tutorial software, both from Data Translation -07839A 1988.

To obtain a calibration curve between the hue value and oil–water content, a two-dimensional calibration chamber, consisting of compartments with known quantities of oil and water, was constructed (Fig. 1). The oil used was Soltrol 220, an isoparaffine solvent composed of a mixture of alkanes C13 through C17 from Phillips 66. The water was colored with FD&C blue #1, at a concentration of 0.005% by weight. By trial and error, the color blue and the specific concentration of 0.005% were found to give the widest range of hue values. The calibration chamber had dimensions of 32.5 cm high, 26 cm wide and 1 cm thick and was divided into six cells of 3 cm high, 26 cm wide and 1 cm thick. The walls consisted of a 1 cm thick Hyzod polycarbonate sheet, made by Sheffield Plastic. All non-soil areas were covered with black tape to avoid edge effects of transmitted light through the plastic walls. The cells were filled with coarse 12/20 sand and water contents of 0, 20, 40, 60, 80 and 100% water saturation (volumetric moisture content of 0.00, 0.07, 0.14, 0.21, 0.28 and 0.35 cm^3/cm^3, respectively). The remainder of the pore space was filled with oil. The coarse 12/20 sand was industrial quartz (Unimin) with particle sizes between 0.85 and 1.5 mm. Many procedures were tried to fill the cells. Consistent results were obtained with the same 35% bulk density as

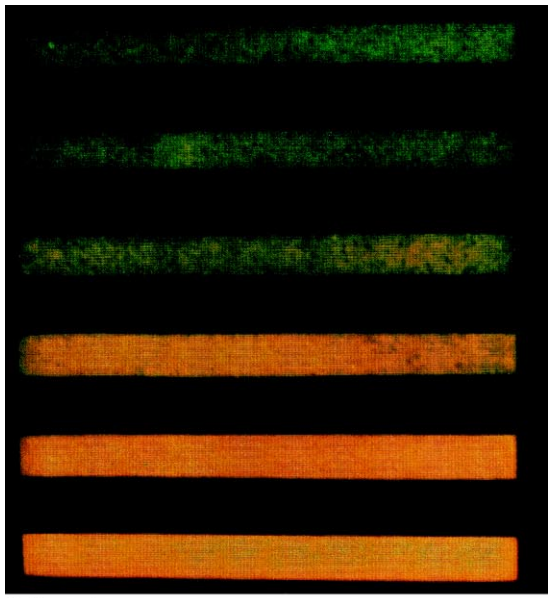

Fig. 1

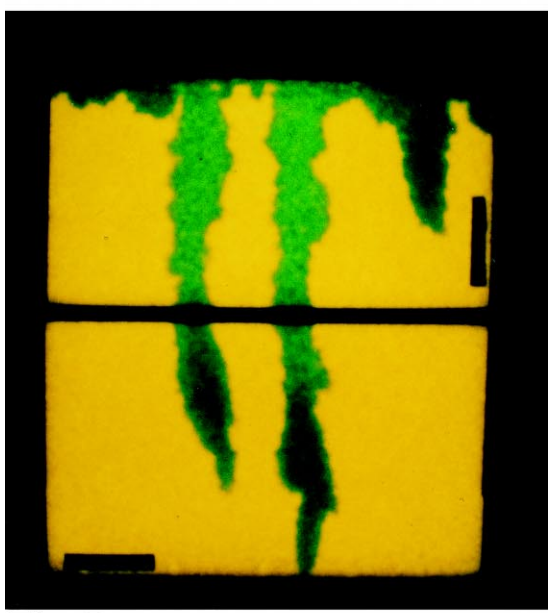

Fig. 5

Fig. 1. Calibration chamber. Water content in the compartments from top to bottom is 0.35, 0.28, 0.14, 0.07, and 0.00 cm^3/cm^3, respectively. Note: The picture does not accurately represent the true colors.

Fig. 5. Water fingering in oil-saturated sand.

in the chamber with the following two procedures: The cells with the 0 and 100% water saturations were filled by dripping fluid into the sand. The 20, 40, 60 and 80% water saturations were obtained by mixing the exact amounts of water, oil and sand in a beaker and loading the mixture in the cells and then packing the cells by vibration.

For each cell, the hue was measured of 100 pixels along a centered horizontal line. A histogram of pixel hue values was made and the mean hue values were calculated for each water content. A calibration curve was obtained by plotting the mean hue value vs. the corresponding water content.

Two types of experiments were conducted to illustrate the reliability and applicability of the method. The first one aimed to test the accuracy of the technique for a simple flow experiment in which the water entered into an oil-saturated 12/20 coarse sand from a point source to check the mass balance. The second experiment illustrated the technique for unstable fingered flow in an oil-saturated sand, similar to the experiment of Rimmer et al. (1998) with synchrotron X-rays. These experiments were carried out in a two-dimensional slab chamber (Fig. 2). The interior dimensions of the experimental chamber were 57 cm high, 51 cm wide and 1 cm thick. Two metal bars at the top and middle of the chamber prevented expansion of the chamber when filled with a fluid. The

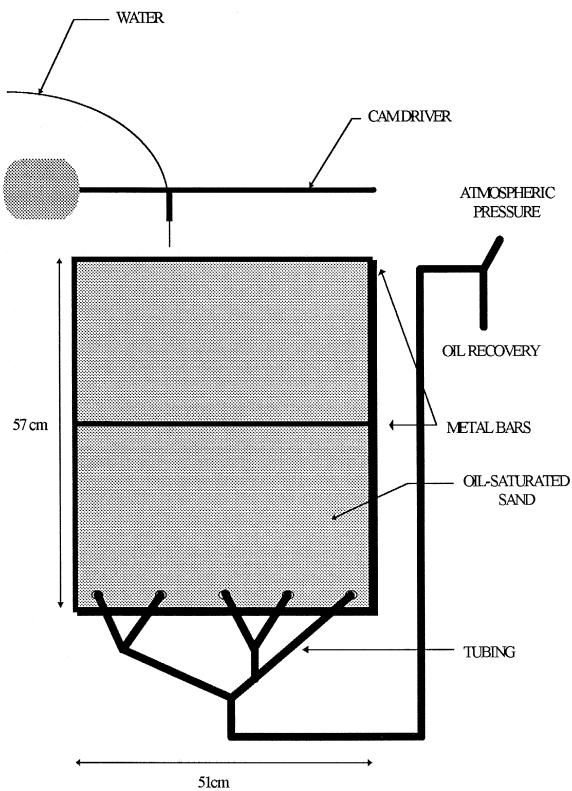

Fig. 2. Experimental chamber.

walls consisted of 1 cm thick Hyzod polycarbonate sheets made by Sheffield Plastic. The experimental chamber was continuously filled with industrial quartz 12/20 sieve size sand through a funnel-extension-randomizer assembly to minimize segregation and heterogeneity (Glass et al., 1989). Extra sand was added to have a 10 cm sand layer in the funnel to achieve an uniform bulk density throughout the chamber. After packing, the top 2 cm of the sand was removed by sweeping to bring the sand height to 55 cm. The experimental chamber was saturated with oil to a height of 55 cm by adding Soltrol from the bottom at a constant rate of 8.4 ml/min. The oil level was kept constant and excess oil was drained through the bottom of the chamber via an overflow at the same level as the Soltrol upper level in the chamber. The experiments were performed at a constant temperature of 20°C.

During the first experiment, 20 ml of water was injected at a flow rate of 2.8 ml/min from a point source located 3 cm below surface of the oil-saturated 12/20 sand. The hue values were taken for all pixels constituting the area surrounding the finger and, subsequently, converted to water content.

In the second experiment, we applied water continuously and uniformly through a needle, attached to a cam driver which went back and forth at a frequency of 8 s, along the top, 1 cm above the surface of oil-saturated 12/20 sand. Fig. 2 depicts the experimental setup. A set of three experiments were performed in the experimental chamber. Fluid content of water fingers was measured for three different infiltration flow rates: 4.5, 7.5 and 10.4 ml/min. The experiment was stopped when the water entered the overflow tube.

4. Results

4.1. Calibration of the light transmission method (LTM)

Color differences were visible between the different cells of the calibration chamber: The oil-saturated cell appeared yellow, the water-saturated cell appeared blue and the oil–water-saturated cells appeared varying shades of green. In each cell, the color was not completely uniform, slight spatial differences existed due to oil and water ganglia formation (Fig. 1).

Inside each cell, the color attributes of pixels were correlated with water content in RGB and HSI formats. Using RGB format, even though the color went from yellow to green to blue, only the red component of the RGB vector showed any trend with water content. This trend, however, was not sufficient to give a unique relationship with water content. The difficulty in using RGB is the interdependence of color saturation with values of the components of the color vector (Wilson, 1988). In our case, the bright yellow (0% water) had approximately the same value for the blue component as the 100% water which was pale blue. Thus, even if the eye can see a difference in color, RGB is unable to pick out the colors in a simple predictable manner. In HSI format, the hue (representing the color for the human eye) is independent of the color saturation (Wilson, 1988). In order to find out if the hue was a better predictor of moisture content,

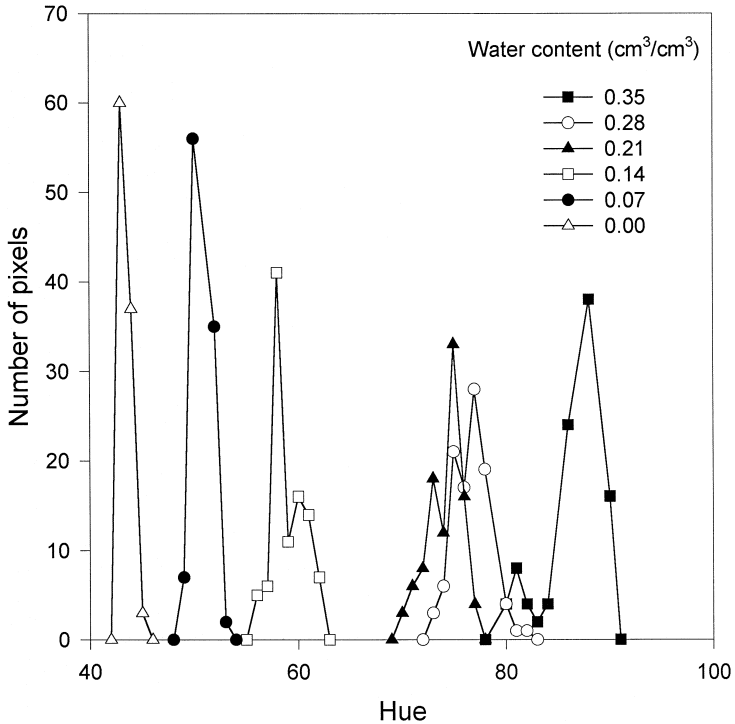

Fig. 3. Hue distribution for different water and oil contents in 12/20 sand.

a histogram of the hue values of each of the 100 pixels for the six different water contents are plotted in Fig. 3. Note that the hue values are integers. Fig. 3 shows that the hue histograms for the different water content in each cell were different. Neither saturation nor intensity had significant correlation to water content (results not shown). The yellow oil-saturated cell had a mean hue value of about 43 and the blue–green water-saturated cell had a mean hue value of about 86. The oil-saturated cells had the most uniform color and the narrowest hue histograms. The histograms of the pixel hue values for the 21% and 28% water content overlapped because of nonuniform distribution of the oil and water, but there was a difference in peak positions and mean hue value. Some of the lower pixel hue values of the water saturated cell also intersected the histogram of the 28% water content.

The mean hue value increased with the water content and a linear regression provided a good fit with an R^2 of 97.8% (Fig. 4). The hue–water content equation is:

$$\theta = -0.9395 + 0.0222\,H \tag{2}$$

where θ is the volumetric water content and H is the hue value calculated with Eq. (1) from the recorded RGB color attributes. Note that the constants in Eq. (2) are specific for our experimental setup. The system needs to be calibrated when different video cameras or particle sizes are used.

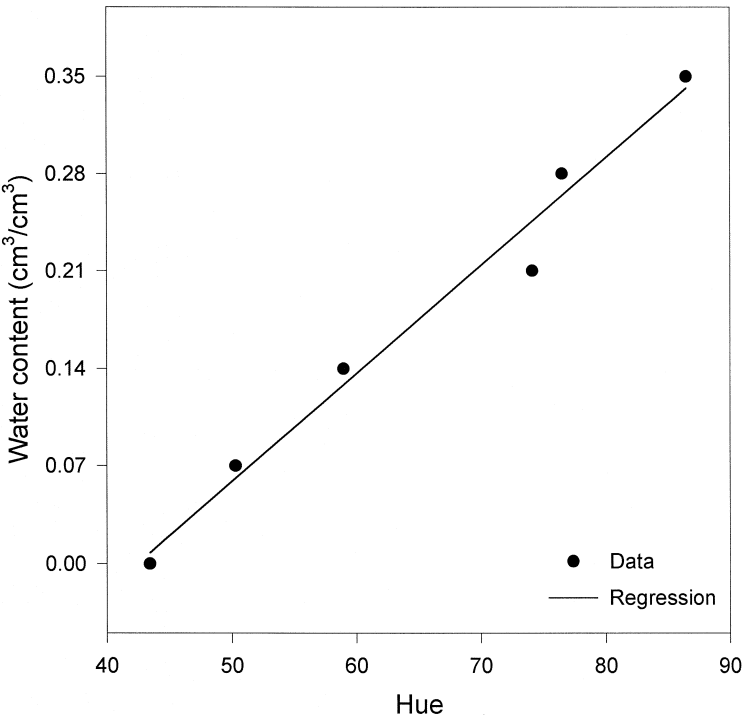

Fig. 4. Plot of average hue vs. water content.

4.2. Accuracy, utility and reliability of LTM

The LTM was evaluated with a mass water balance and synchrotron X-ray technique. The mass balance test consisted of measuring a known water volume in oil-saturated sand. The injected 20 ml of water generated a finger of dimensions approximately 10 cm long, 6 cm wide and 1 cm thick in the experimental chamber. Hue values were obtained by analyzing all the 14 400 pixels present in a surrounding area that contains the finger and were converted to water content values using Eq. (2). The total amount of water calculated was 19.85 ml, which was within 1% of the amount of water applied.

As an application and to check the accuracy of LTM under transient flow conditions, water was continuously applied on 12/20 oil-saturated sand. Three different flow rates were used. In each case, an unstable wetting front was formed resulting in one or more fingers. An example of the fingered flow of water for the application rate of 4.5 ml/min is presented in Fig. 5. Before the first finger went down, a horizontal wetting front of about 2 cm formed. The finger was the bluest (highest value for hue) at the tip, indicating the highest water content. This is similar for water fingers in air dry sand. Fig. 6 shows the finger water content profile after 15 and 20.5 min LTM measurements indicated that after 15 min the maximum water content near the finger tip was between 0.27 and 0.30 cm^3/cm^3 and the finger width ranged from 6 to 8 cm. At 20.5 min, the

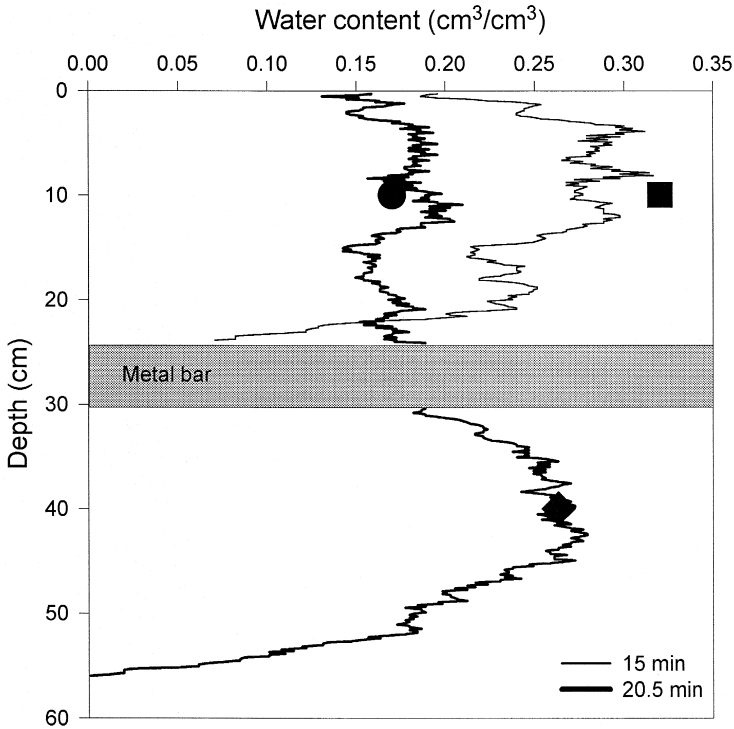

Fig. 6. Vertical water finger profiles using light transmission method at two different times. The finger has a wet tip and drier tail. The large symbols are moisture contents from similar experiments using X-ray attenuation. The square and diamond are at the finger tip at two different depths and the circle is in the tail at 10 cm depth.

maximum water content near the finger tip was between 0.26 and 0.28 cm^3/cm^3. At approximately 25 cm above the finger tip, the moisture content decreased to an average of 0.17 cm^3/cm^3. The horizontal water content profile at a depth of 48 cm at 20.5 min through the tip of the finger is shown in Fig. 7. Both infiltration flow rates of 7.5 and 10.5 ml/min produced a wetting front instability that generated 2 and 3 fingers, respectively, with approximately the same characteristics as the one generated with 4.5 ml/min. The only difference was that the water content was slightly higher and the velocities sometimes slower (Table 1).

The above results were compared with available data from synchrotron X-ray measurements by Rimmer et al. (1998) with 12/20 oil-saturated sand and a flow rate of 2.3 ml/min through a point source (Fig. 6). For the synchrotron measurements, unlike LTM, there is a fundamental relationship between the attenuation of X-rays and moisture content. Although slight differences existed in observed water contents, which may have been caused by slightly different experimental flow rates, both methods follow the same finger behavior. The highest water content was measured near the finger tips: 0.265 cm^3/cm^3 for the X-ray radiation and 0.26 to 0.28 cm^3/cm^3 for the LTM (Fig. 6). Although the wetting front at the finger tip was slightly sharper for the X-ray

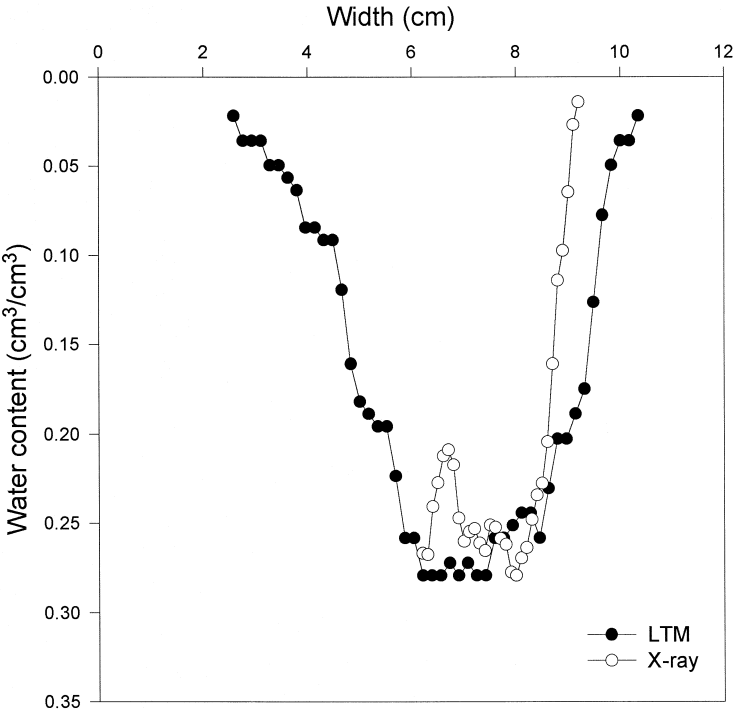

Fig. 7. Horizontal water finger profile at a permanent location (47.6 cm depth for LTM and 30 cm depth for X-ray). LTM infiltration rate is 4.5 ml/min. X-ray infiltration rate is 2.3 ml/min.

measurement than for the LTM, the decrease in water content in the transition zone above the maximum water content is similar over the zone that the synchrotron was available. In Fig. 7, the moisture content in a horizontal profile at comparable locations over which the X-ray measurements were available, was also very similar between the two methods.

Table 1
Water fingers characteristics

Pure water experiments (ml/min)	Number of fingers	Average width (cm)	Average velocity (cm/min)	Maximum water content
4.5	1	6–8	5.7	0.27
7.5	2	5–6	#1, 3.95	#1, 0.20–0.30
			#2, 4.48	#2, 0.25–0.30
10.4	3	6	#1, 5.6	#1, 0.25–0.30
			#2, 6.0	#2, 0.25–0.30
				#3, 0.30

5. Discussion

The Light Transmission Method was found to yield reliable fluid contents in transient oil–water flow fields as checked by the mass conservation experiment. Unstable fingered flow phenomena measured with LTM gave similar results as those with the synchrotron X-ray source. The advantage of the LTM is that it records the fluid contents of the whole flow field in less than 0.05 s (the time it takes for a video camera to take an image). Synchrotron X-ray measurements can also be taken within 1 s but only at one location at a time. The disadvantage of LTM is that silica sand has to be used as porous media while synchrotron X-ray measurements are independent of the translucence of the porous media. Another requirement for the LTM is that the slab of soil has to be relatively thin, effectively making it 2-D. For unstable flow fields, previous experiments have shown that 2-D fingers can be scaled to 3-D fingers. The width for example can be scaled by a factor $4.18/\pi$ (Glass et al., 1991). The LTM when coupled with simultaneous pressure measurements will be useful in validating 1-D and 2-D computer codes for transient oil and water flow.

6. Conclusions

A method was developed that can measure full flow field average fluid contents for transient flows in soil–oil–water systems. Currently, there is a lack of such measuring techniques, hampering the development of theory and testing of two-phase models.

We found that by dying the water light blue and analyzing the flow field for this blue color in HSI format, we could determine the water content in the slab chamber filled with sand. RGB, which is used in recording color with video cameras, could not easily quantify the obvious color difference between yellow and blue. By using the HSI format, a unique relationship existed between the hue and water content. Comparison with moisture contents, determined with synchrotron X-rays, showed that the LTM can be used for 2-D flow field moisture contents in porous media consisting of silica sand.

Acknowledgements

This work was sponsored by the U.S. Air Force Office of Scientific Research, under Grant No. F49620-94-1-0291.

References

Chuoke, R.L., van Meurs, P., van der Poel, C., 1959. The instability of slow, immiscible viscous, liquid–liquid displacement in permeable media. Petrol. Trans. AIME 216, 188–194.

Dane, J.H., Oostrom, M., Missildine, B.C., 1992. An improved method for the determination of capillary pressure-saturation curves involving TCE, water and air. J. Contam. Hydrol. 11, 69–89.

Glass, R.J., Nicholl, M.J., 1995. Physics of gravity fingering of immiscible fluids within porous media: An overview of current understanding and selected complicating factors. Geoderma 70 (2–4), 133–163.

Glass, R.J., Steenhuis, T.S., Parlange, J.-Y., 1989. Mechanism for finger persistence in homogeneous, unsaturated, porous media: Theory and verification. Soil Sci. 148 (1), 60–70.

Glass, R.J., Parlange, J.-Y., Steenhuis, T.S., 1991. Immiscible displacement in porous media: Stability analysis of three-dimensional, axisymmetric disturbances with application to gravity-driven wetting front instability. Water Resour. Res. 27 (8), 1947–1956.

Hopmans, J.W., Dane, J.H., 1986. Calibration of a dual-energy gamma radiation system for multiple point measurements in a soil. Water Resour. Res. 7, 1009–1114.

Illangasekare, T.H., Ramsey, J.L. Jr., Jensen, K.H., Butts, M.B., 1995. Experimental study of movement and distribution of dense organic contaminants in heterogeneous aquifers. J. Contam. Hydrol. 20, 1–25.

Lenhard, R.J., Dane, J.H., Parker, J.C., Kaluarchchi, J.J., 1988. Measurement and simulation of one-dimensional transient three-phase flow for monotonic liquid drainage. Water Resour. Res. 24 (6), 853–863.

Liu, Y., Bierck, B.R., Selker, J.S., Steenhuis, T.S., Parlange, J.-Y., 1993. High intensity X-ray and tensiometer measurements in rapidly changing preferential flow fields. Soil Sci. Soc. Am. J. 57, 1188–1192.

Mercer, J.W., Cohen, R.M., 1990. A review of immiscible fluids in the subsurface: Properties, models characterization and remediation. J. Contam. Hydrol. 6, 107–163.

Rimmer, A., DiCarlo, D.A., Steenhuis, T.S., Bierck, B., Durnford, D., Parlange, J.-Y., 1998. Rapid fluid content measurement method for fingered flow in an oil-water-sand system using synchroton X-rays. J. Contam. Hydrol. 31, 315–334.

Saffman, P.G., Taylor, G., 1958. The penetration of a fluid into a porous medium or Hele–Shaw cell containing a more viscous liquid. Proc. R. Soc. London A 245, 312–331.

Schwille, F., 1988. Dense Chlorinated Solvents in Porous and Fractured Media (J.F. Pankow, Trans.). Lewis Publishers, Chelsea, MI, 146 pp.

Tidwell, V.C., Glass, R.J., 1994. X-ray and visible light transmission for laboratory measurements of two-dimensional saturation fields in thin-slab systems. Water Resour. Res. 30, 2873–2882.

Van Geel, P.J., Sykes, J.F., 1994. Laboratory and model simulations of a LNAPL spill in a variably-saturated sand: 1. Laboratory experiment and analysis technique. J. Contam. Hydrol. 17, 1–25.

Wilson, A., 1988. What color is color? The Electronic System Design Magazine, January, pp. 38–44.